

Impact of elongated orientations in the decay dynamics of ^{252}Cf nucleus

Chahat Jindal* and Manoj K. Sharma

Department of Physics and Material Science

Thapar Institute of Engineering and Technology, Patiala-14007, Punjab, INDIA

1. Introduction

The nuclei belonging to heavy mass region may decay via α -decay, cluster decay, heavy particle radioactivity etc. Understanding of these processes is essential for gaining insights of the nuclear stability and the decay mechanisms. Literature suggests that the ^{252}Cf nucleus may disintegrate through both binary [1] and ternary [2] fission processes. Among these, binary fission is more commonly observed and the asymmetric fission fragments are observed in this channel. Experimental evidence [1] has shown that the fission path of such nuclei is characterized by the magic shell closure, which is indicative of the enhanced nuclear stability of the decaying fragments. Based on different nuclear properties, various theoretical approaches have been introduced in view of binary and ternary decay of ^{252}Cf nucleus. To accurately model the interaction potential among fission fragments and gain a deeper understanding of nuclear decay processes, two primary approaches are commonly used: the proximity potential and the Skyrme-based potential. In the present work, binary fission fragmentation of ^{252}Cf is analyzed using the Quantum Mechanical Fragmentation Theory (QMFT). Additionally, the role and significance of nuclear potentials, such as the proximity and Skyrme based potentials, is explored in the context of ^{252}Cf decay dynamics, offering a comparative understanding of these interactions in predicting the fission outcomes.

2. Methodology

In the present work, the fragmentation analysis is carried out using QMFT. The fragmen-

tation potential is calculated as in:

$$V_R(\eta, R) = \sum_{i=1}^2 B(A_i, Z_i) + V_C(R, Z_i, \beta_{\lambda_i}, \theta_i) + V_P(R, A_i, \beta_{\lambda_i}, \theta_i) \quad (1)$$

Here, $B(A_i, Z_i)$ represents the binding energies of the fission fragments, while V_C refers to the Coulomb potential, and V_P corresponds to the short-range nuclear potential. The binding energies and deformation parameters are adopted from the mass table [3]. For the short-range nuclear potential V_P , both the proximity potential [4] and a potential derived from the energy density formalism (EDF) [5] are employed. For proximity potential ref to [4]. Additionally, the nucleus-nucleus interaction potential based on EDF method is defined as [5]

$$V_P(R) = E(R) - E(\infty) \quad (2)$$

Here, $E = \int \{H(r)\} d\vec{r}$, where H is Skyrme Hamiltonian.

3. Results and discussion

Firstly the fragmentation potential governing the binary decay of the ^{252}Cf nucleus is analysed and plotted in Fig. 1, as a function of fragment mass number A_2 . Calculations are performed for both spherical and elongated configurations to understand the decay characteristics in different geometrical arrangements. Fig. 1 reveals that a near symmetric mass distribution is favored for the spherical configuration, particularly yielding fragments such as ^{122}Cd and ^{130}Sn ($Z = 50$, $N = 80$). This suggests that the spherical shape leads to near symmetric fission, producing fragments around the magic shell closure. Conversely, the elongated configuration leads to a double

*Electronic address: cchahat_phd21@thapar.edu

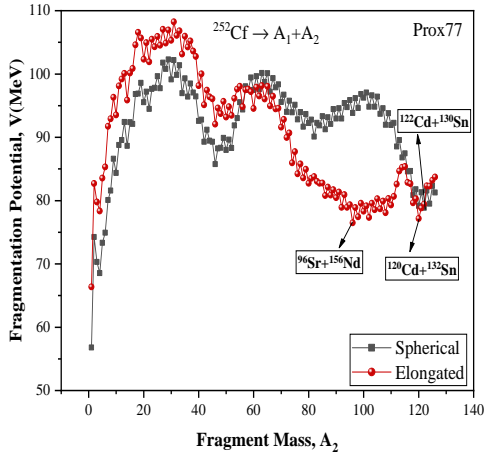


FIG. 1: Fragmentation potential of ^{252}Cf nucleus plotted with respect to the fragment mass A_2 .

humped fission fragment distribution, resulting in pairs such as $^{120}\text{Cd} + ^{132}\text{Sn}$ ($Z = 50$, $N = 82$) and ^{96}Sr ($Z=38$, $N=58$) + ^{156}Nd ($Z = 60$, $N = 96$) respectively. These results indicate that symmetric fragments are favoured at spherical magic shell closure ($Z = 50$, $N = 82$) and asymmetric fragments near deformed magic shell ($Z = 38$, $N = 60$), emphasizing the role of nuclear shell effects in determining the fragment mass distributions. Furthermore, the mass fragmentation obtained from the elongated configurations show reasonable agreement with experimental data. However, the half-life of these fragments could-not be addressed in the scope of proximity potential. This may be due to the reason that the barrier decreases significantly due to increase in the interaction radius for the elongated configuration.

Therefore, an attempt is made to address this issue by incorporating nuclear potential based on the Skyrme energy density formalism (SEDF). It was observed that there was still lowering in the barrier characteristics for

skyrme forces such as SIII, GSKI etc. Therefore, further analysis was conducted by exploring Skyrme forces imparting a higher potential

TABLE I: The PCM-calculated half-life for spontaneous fission along with fitted neck-length parameter ΔR are presented using SKT3 force.

Parent nucleus	Decay channel	ΔR (fm)	$\log_{10}T_{1/2}^{SF}$ (Exp.)	$\log_{10}T_{1/2}^{SF}$ (PCM)
Spherical				
^{252}Cf	$^{122}\text{Cd} + ^{130}\text{Sn}$	0.125	9.43 ± 0.01	9.04
Deformed				
^{252}Cf	$^{108}\text{Mo} + ^{144}\text{Ba}$	-0.295	9.43 ± 0.01	9.31

barrier, such as the SKT2 and SKT3 [6] parameter set. Eventually, SKT3 force was employed to get the optimum barrier characteristics. The calculations done using the SKT3 parameter set give a good account of the half-lives, as evident from Table 1. The identified most probable fission fragments for spherical as well as a elongated choice of fragments are also shown in Table 1. We are in the process of investigating the relevance of Skyrme-based interactions in the context of the ternary fission of ^{252}Cf .

References

- [1] L. E. Geendenin *et al.*, J. Inorg. Nucl. Chem., **1**, 45 (1995).
- [2] A. V. Ramayya *et al.*, Phys. Rev. C **57**, 2370 (1998), K. Manimaram *et al.*, J. Phys. G: Nucl. Part. Phys. **37**, 045104 (2010).
- [3] P. Moller *et al.*, At. Data Nucl. Data Tables **109**, 1 (2016).
- [4] J. Blocki, *et al.*, Ann. Phys. **105**, 427 (1977).
- [5] M. Beiner, *et al.*, Nucl. Phys. A **238**, 29 (1975).
- [6] I. Sharma, *et al.*, Nucl. Phys. A **983**, 276 (2019).